PNAS RESEARCH ARTICLE | GENETICS OPEN ACCESS

APOBEC2 safeguards skeletal muscle cell fate through binding chromatin and regulating transcription of non-muscle genes during myoblast differentiation

J. Paulo Lorenzo[a,b,1], Linda Molla[c,1], Elias Moris Amro[a,1], Ignacio L. Ibarra[d,e], Sandra Ruf[a], Cedrik Neber[a], Christos Gkougkousis[a], Jana Ridani[f,g], Poorani Ganesh Subramani[f,g], Jonathan Boulais[f], Dewi Harjanto[c], Alin Vonica[h], Javier M. Di Noia[f,g,i], Christoph Dieterich[j,k], Judith B. Zaugg[d], and F. Nina Papavasiliou[a,b,c,2]

Edited by Helen Blau, Stanford University, Stanford, CA; received July 25, 2023; accepted March 7, 2024

The apolipoprotein B messenger RNA editing enzyme, catalytic polypeptide (APOBEC) family is composed of nucleic acid editors with roles ranging from antibody diversification to RNA editing. APOBEC2, a member of this family with an evolutionarily conserved nucleic acid–binding cytidine deaminase domain, has neither an established substrate nor function. Using a cellular model of muscle differentiation where APOBEC2 is inducibly expressed, we confirmed that APOBEC2 does not have the attributed molecular functions of the APOBEC family, such as RNA editing, DNA demethylation, and DNA mutation. Instead, we found that during muscle differentiation APOBEC2 occupied a specific motif within promoter regions; its removal from those regions resulted in transcriptional changes. Mechanistically, these changes reflect the direct interaction of APOBEC2 with histone deacetylase (HDAC) transcriptional corepressor complexes. We also found that APOBEC2 could bind DNA directly, in a sequence-specific fashion, suggesting that it functions as a recruiter of HDAC to specific genes whose promoters it occupies. These genes are normally suppressed during muscle cell differentiation, and their suppression may contribute to the safeguarding of muscle cell fate. Altogether, our results reveal a unique role for APOBEC2 within the APOBEC family.

APOBEC family | transcriptional regulator | DNA binding | muscle differentiation | safeguard factor

The apolipoprotein B messenger RNA editing enzyme, catalytic polypeptide (APOBEC) proteins are zinc-dependent deaminases that catalyze the removal of the amino group from a cytidine base in the context of a polynucleotide chain, resulting in cytidine (C) to uridine (U) transition on DNA or RNA. Members of the APOBEC family are closely related to one another based on homology and conservation of the cytidine deaminase domain containing a zinc-dependent deaminase sequence motif (1). However, they differ by tissue-specific expression, substrates, and biological functions (reviewed in ref. 2). Physiologically this deaminase family alters the informational content encoded in the genome through a range of processes: editing messenger RNA (mRNA) to affect translation, e.g., APOBEC1 (3, 4), mutating DNA to create novel gene variants, restrict viruses and retrotransposons, e.g., AICDA (AID) and APOBEC3 (reviewed in ref. 5) and, changing DNA 5mC modification levels to modulate transcript abundance, e.g., AID (6, 7).

APOBEC2 is an evolutionarily conserved member of the APOBEC family. It retains the characteristic conserved cytidine deaminase domain and together with AID is under strong purifying selection (8, 9). Substantial evidence highlights the biological relevance of APOBEC2. In mice, APOBEC2 is highly expressed in cardiac and skeletal muscle where it affects muscle development (10, 11). Specifically, in the absence of APOBEC2, there is a shift from fast to slow muscle fiber formation, a reduction in muscle mass, and a mild myopathy with age (12). In zebrafish, APOBEC2 has also been implicated in skeletal muscle and cardiac muscle physiology (13) and in retina and optic axon regeneration (14). In frogs, APOBEC2 is important in left–right axis specification during early embryogenesis (15). Mutations and gene expression changes of APOBEC2 have also been linked to cancer development (16–18).

Even though there is evidence for a biological role of APOBEC2, there are few insights to the molecular mechanism by which APOBEC2 accomplishes these. Moreover, there has been no definite demonstration of its activity as a cytidine deaminase. Based on its homology with the other APOBEC family members, it is hypothesized that APOBEC2 may be involved in RNA editing (11, 18) or DNA demethylation (14, 19, 20). Alternatively, APOBEC2 may have lost its deaminase activity altogether and may act biologically by a different mechanism (21). However, the direct molecular substrate, if it exists, for APOBEC2 remains to be identified.

Significance

The apolipoprotein B messenger RNA (mRNA) editing enzyme, catalytic polypeptide (APOBEC) family comprises cytidine deaminases with diverse roles in human immunity. These deaminases alter DNA or RNA nucleotides that affect human physiology, antibody diversification, and innate immunity. APOBEC2, however, had neither a defined role nor an established molecular function. We uncover a unique role for APOBEC2 in transcriptional regulation. We show that it binds specific motifs within gene promoters, and at the same time, it interacts with the histone deacetylase complex, which is involved in transcriptional repression through histone modification. Because the genes that are repressed are involved in the specification of non-muscle cell fates, our work suggests that APOBEC2 plays a role in cell fate specification.

The authors declare no competing interest.

This article is a PNAS Direct Submission.

[1]J.P.L., L.M., and E.M.A. contributed equally to this work.

[2]To whom correspondence may be addressed. Email: n.papavasiliou@dkfz-heidelberg.de.

This article contains supporting information online at https://www.pnas.org/lookup/suppl/doi:10.1073/pnas.2312330121/-/DCSupplemental.

Published April 16, 2024.

To address this, here, we performed knockdown studies of APOBEC2 during the differentiation of the C2C12 murine skeletal myoblast cell line to systematically characterize the transcriptome and DNA methylation patterns of APOBEC2-deficient C2C12 cells. Our results confirm the requirement of APOBEC2 for myoblast to myotube differentiation. While our results neither supported APOBEC2 roles on RNA editing nor on DNA methylation, we found that APOBEC2 reduction led to substantial gene expression changes affecting programs associated with myogenesis. Moreover, genomic occupancy experiments demonstrated that APOBEC2 interacts with chromatin at promoters of transcriptionally regulated genes during myoblast differentiation. Notably, these APOBEC2-occupied target genes were not directly involved in muscle differentiation but were rather mostly transcriptional regulators of nonskeletal muscle fates, e.g., immune cell differentiation. Finally, our findings indicating the direct binding of DNA by APOBEC2 and its interaction with Histone Deacetylase 1 (HDAC1) corepressor complexes at specific promoter regions provide the underlying mechanism of its function to safeguard muscle cell fate.

Results

APOBEC2 Is Required for Myoblast to Myotube Differentiation. The initial motivation for this work came from the observation of the cross-section of tibialis anterior (TA) muscles from 10-wk-old APOBEC2-deficient, *Apobec2*−/−, (A2KO) mice which had increased incidence of centrally nucleated myofibers (Fig. 1 *A* and *B*). Centrally nucleated fibers arise from activation of peripheral muscle satellite cells usually in response to injury (22). This phenotype may indicate disrupted or stalled muscle differentiation of the muscle satellite cells as these mice have not been experimentally injured. A similar phenotype was observed

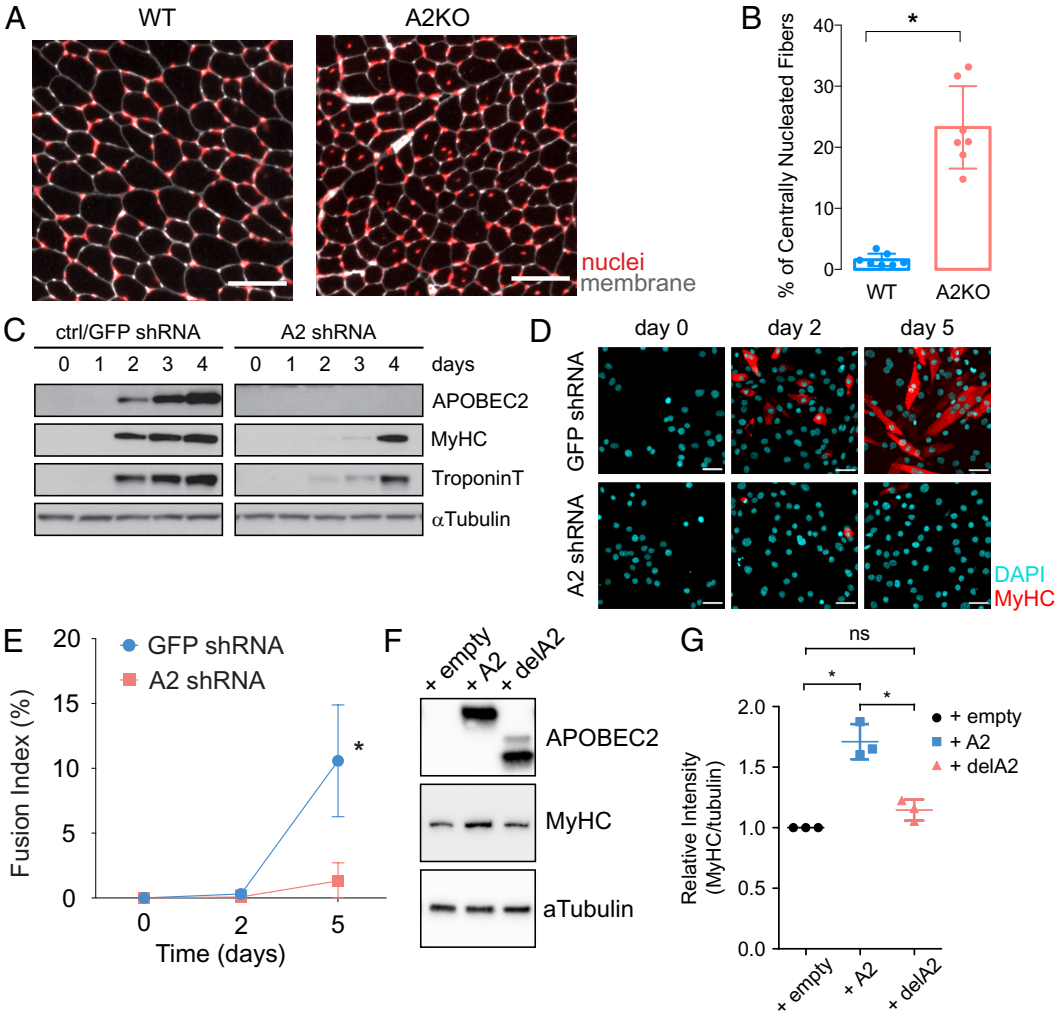

Fig. 1. APOBEC2 loss affected muscle homeostasis in vivo and muscle differentiation in vitro. (*A*) Staining of TA muscle cross-sections of age-matched wild-type and APOBEC2 KO (A2 KO) mice. Sections were stained with wheat germ agglutinin for cell membranes (WGA, gray) and DAPI for nuclei (red). (Scale bar, 200 μm.) (*B*) Quantification of the percentage of centrally nucleated fibers in WT and A2 KO TA cross-sections. Bar plots represent the mean and SD measured from seven animals per condition; *$P < 0.05$. (*C*) Western blot of cell lysates from C2C12 cell lines, GFP shRNA and A2 shRNA, at different timepoints of myoblast differentiation (day 0 to day 4). C2C12 myoblasts were transduced either with shRNA against GFP (GFP shRNA) or shRNA against APOBEC2 (A2 shRNA). MyHC, and TroponinT were used as markers of late differentiation; αTubulin, as loading control. (*D*) Immunostaining of C2C12 cell lines, GFP shRNA and A2 shRNA, at different timepoints of myoblast differentiation (day 0 to day 5). Samples were stained using an antibody specific to MyHC (red) and DAPI (cyan). (Scale bar, 50 μm.) (*E*) Quantification of fusion indices of C2C12 cell lines, GFP shRNA and A2 shRNA, at different time points of myoblast differentiation (day 0 to day 5). Fusion index represents the ratio of multinucleated cells (≥2 nuclei). The line plot corresponds to the mean values of the fusion index at each time point from three replicates with six fields of view each; *$P < 0.05$. (*F*) C2C12 knockdown cell line (A2 shRNA) was transduced with retrovirus overexpressing APOBEC2 or empty vector control (+ empty: transduced with empty vector, +A2: with APOBEC2 vector, and +delA2 with truncated APOBEC2). Cells were collected 96 h posttransduction. Cell lysates were prepared and analyzed by western blot. Representative blot from three independent biological replicates. (*G*) Quantification of MyHC intensity from western blots. Corresponding points represent the ratio of MyHC to αTubulin mean intensity; each point was normalized to the corresponding empty control (+ empty) sample for each trial. Dot and whisker plots represent the mean (n = 3). Whiskers represent the SD; ns = $P > 0.05$; * = $P < 0.05$.

in another APOBEC2 knockout mouse model; however, it was only evident in aged mice (12). We hypothesized that APOBEC2 may have an undescribed molecular function in the maintenance of muscle homeostasis or muscle satellite cell quiescence.

To unravel this molecular function, we used the C2C12 myoblast cell line that was derived from mouse satellite cells (23, 24). These cells recapitulate the first steps of muscle differentiation in culture and upon differentiation induce APOBEC2 expression (15) (validated in *SI Appendix*, Fig. S1 *A* and *B*). To explore the role of APOBEC2 during myogenesis, we reduced APOBEC2 protein levels with short hairpin RNA (shRNA) against APOBEC2 mRNA. APOBEC2 protein reduction coincided with decreased myoblast to myotube differentiation, evidenced by decreased protein levels of TroponinT and myosin heavy chain (MyHC) (Fig. 1*C*). At the cellular level, downregulation of APOBEC2 protein levels coincided with reduced myotube formation (Fig. 1 *D* and *E*). These observations match those previously reported using mouse embryonic stem cell–derived myogenic precursors (25).

We then restored APOBEC2 protein in these knockdown cells through expression of a codon-switched shRNA-resistant version. APOBEC2 restoration led to an increase in MyHC protein levels (Fig. 1 *F* and *G*). This confirmed the essential and direct role of APOBEC2 in myoblast differentiation in vitro and provided a mechanism to the disrupted differentiation observed in the A2KO mouse models. Additionally, we produced truncated APOBEC2 (residues 41 to 224 mouse APOBEC2), which lacks the amino-terminal (N-terminal) region of APOBEC2 (26), a flexible disordered region hypothesized to be involved in intermolecular interactions (27). Truncated APOBEC2 (delA2), was unable to restore MyHC protein levels (Fig. 1*G*). Interestingly, it localized exclusively in the cytoplasmic fraction of differentiated C2C12 myoblasts (*SI Appendix*, Fig. S1*C*), suggesting that nuclear localization of APOBEC2, mediated by its disordered N-terminal region, might be necessary for its role in muscle differentiation.

APOBEC2 Loss Led to Gene Expression Changes Related to Muscle Differentiation. To study how APOBEC2 loss leads to problems in C2C12 myoblast to myotube differentiation, we performed RNA sequencing (RNA-Seq) to compare the transcriptome dynamics of APOBEC2 knockdown and control cells during differentiation. We observed that reduced APOBEC2 levels led to substantial gene expression changes prior to differentiation (day 0) and early into myotube differentiation (days 1 and 2) (Fig. 2*A* and Dataset S1). Notably, genes with decreased expression across the timepoints were involved in muscle cell development and differentiation (Fig. 2*B* and Dataset S2). The genes with increased expression on the other hand were enriched for Gene Ontology (GO) terms related to nonskeletal muscle processes such as immune cell differentiation, myeloid and T cells, particularly at days 1 and 2 of differentiation (Fig. 2*C* and Dataset S2). The decreased expression of muscle differentiation–related genes directly reflected the observed reduction in myoblast to myotube differentiation. However, the increase in nonmuscle genes was intriguing.

Though undetectable on an immunoblot (Fig. 1*C*), reduction of APOBEC2 mRNA levels prior to inducing differentiation, day 0, affected the potential of C2C12 to differentiate into myotubes. Muscle-related genes were already at a lower mRNA level concomitant with *Apobec2* expression levels. *Akap6* mRNA levels were already reduced at day 0 prior to reduction of genes involved in muscle differentiation, like *Klf4*, *Sox11*, *Tnnt3,* and *Myh1* (Fig. 2 *A* and *D*). *Akap6* is directly involved in muscle homeostasis and differentiation (28, 29). Other such genes involved in muscle system processes were already decreased at day 0 (Dataset S2), potentially reflecting a perturbed myoblast cell fate.

At days 1 and 2, genes involved in nonskeletal muscle pathways showed increased expression (day 1 and 2, Fig. 2*C*). Among these genes are transcription factors, e.g., *Gata3*, *Stat1,* and *Cebpa,* that have roles in cell differentiation (Fig. 2 *A* and *D*) and genes like *Id3* which directly inhibits skeletal muscle differentiation and whose increased expression would explain decreased myotube formation (30). Additionally, genes involved in calcium homeostasis particularly in muscle, *Pde1a* and *Akap6,* also have disrupted mRNA levels (31, 32). The upregulation of spurious nonskeletal muscle programs at day 1 and day 2, and the reduction of muscle-related genes at day 0 or steady-state could reflect a confused muscle cell identity (33).

We next wondered how reduction in APOBEC2 led to gene expression changes. Due to the conserved cytidine deaminase domain within the APOBEC family, APOBEC2 is posited to be an RNA editor (18) and has also been proposed to function as a DNA demethylase (20). Upon comparing the transcriptomes of the APOBEC2 knockdown and control C2C12 cells for instances of C-to-U RNA editing, using a previously validated pipeline (34), we could not identify C-to-U (or A-to-I) RNA editing events that were APOBEC2 dependent (*SI Appendix*, Fig. S2*A*). Similarly, using bisulfite sequencing, we were unable to observe significant methylation differences between the APOBEC2 knockdown and control C2C12 cells that could account for the gene expression changes (*SI Appendix*, Fig. S2 *B* and *C*). Altogether, these results strongly indicate that APOBEC2 is neither involved in RNA deamination nor DNA demethylation in differentiating muscle.

APOBEC2 Occupies Promoter Regions during Myoblast Differentiation. Cytidine deaminases of the APOBEC family can bind and mutate DNA either at gene bodies, e.g., exons of the immunoglobulin locus, as catalyzed by AID, reviewed in ref. 35 or at promoter regions, e.g., local hypermutations as catalyzed by APOBEC3 family members (reviewed in ref. 36). To assess whether APOBEC2 could also bind genomic DNA and affect transcription, we first determined the subcellular localization of APOBEC2 in muscle cells. APOBEC2 was present in both the cytoplasm and nucleus of differentiated C2C12 myotubes (Fig. 3*A* and *SI Appendix*, Fig. S1*C*). Although a weak nuclear localization signal (NLS) was predicted by cNLS Mapper (37) (APOBEC2 residues 26 to 57, with a score of 3.7), APOBEC2 does not show NLS activity but is homogeneously distributed throughout the cell (38).

To then assess whether nuclear APOBEC2 could bind chromatin, we utilized sequential salt extraction based on the principle that loosely bound proteins would dissociate from chromatin at low salt concentration, while tightly bound ones would not (39). Using this technique, we found that a fraction of APOBEC2 within differentiating C2C12 cells was bound to chromatin and washed off at higher salt concentrations (Fig. 3*B*). Interestingly, histone H4, a component of the nucleosome, dissociates completely from DNA at 0.75 M NaCl, while APOBEC2 together with nuclear lamin B and beta-actin, components of the nuclear cytoskeleton, remained associated to the chromatin in up to 1.5 M NaCl. These data suggest a strong association of nuclear APOBEC2 with chromatin and the nuclear cytoskeleton, with potential roles in transcriptional regulation (40).

To determine the location of bound APOBEC2 within chromatin, we performed chromatin immunoprecipitation-sequencing (ChIP-Seq) experiments, and calculated enrichment of APOBEC2 at specific loci over input using MACS2 (41, 42). We performed each experiment in triplicate, and only peaks that were called in at least 2 out of three replicates were analyzed. Importantly, we queried APOBEC2 occupancy at two different time points, 14 and 34 h postdifferentiation, that precede the RNA-Seq time points, where we observed changes in gene expression and represent time points

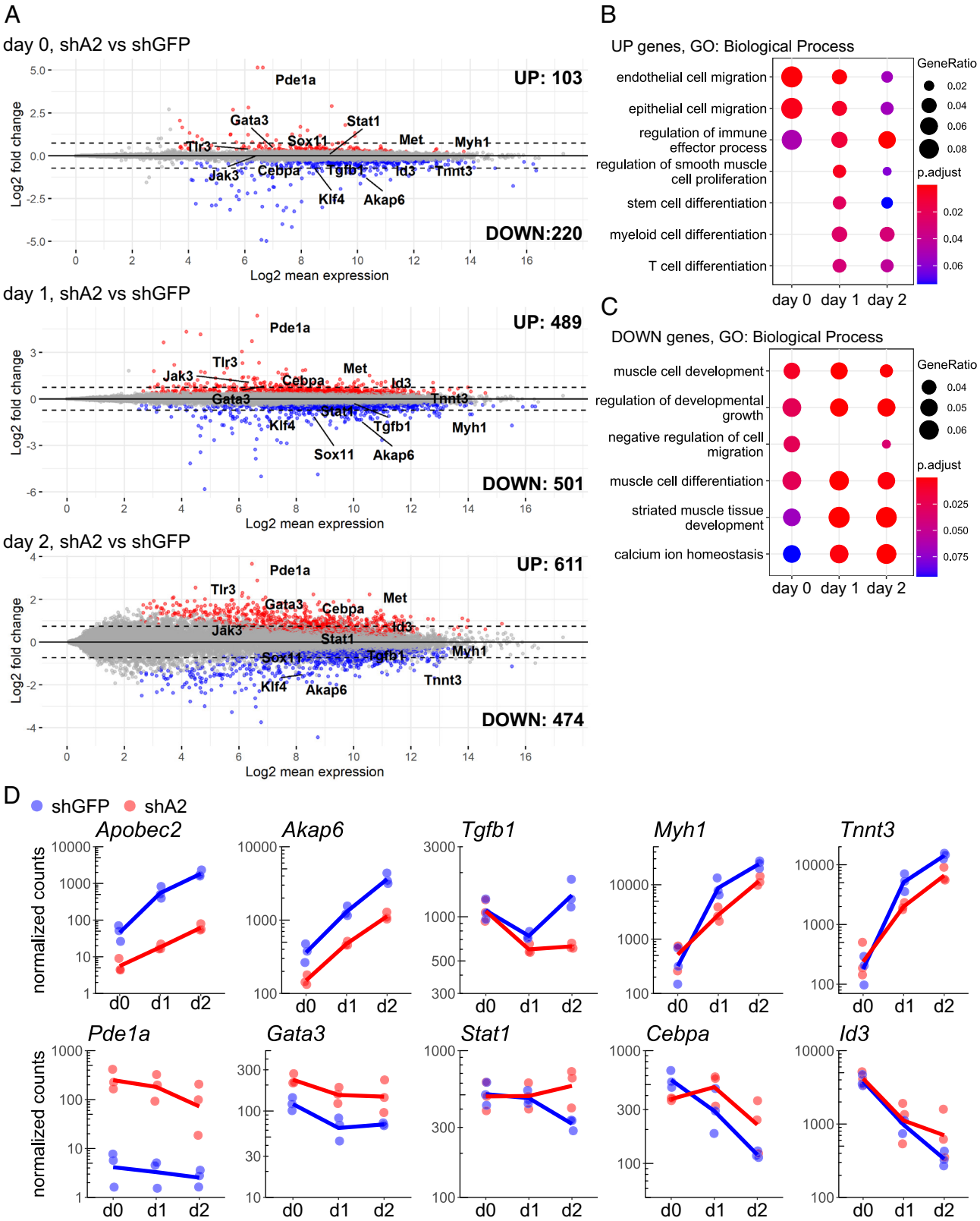

Fig. 2. Gene expression changes due to *Apobec2* knockdown reflected a decrease in muscle formation and an increase in non-muscle-related processes. (*A*) MA plots were generated using log2 fold changes and log2 mean expression values from comparing gene expression differences due to *Apobec2* knockdown (shA2 vs. shGFP) prior to differentiation induction (day 0) and postdifferentiation induction (day 1 and day 2). Labeled points represent *Apobec2* and several differentially expressed genes. Points are colored corresponding to cutoff values for *P*-adjusted (<0.05) and fold change value, red for positive fold change and blue for negative fold change; gray points fall above of *P*-adjusted cutoff. Broken lines represent the log2 FoldChange cutoff at ±0.6. (*B* and *C*) Gene ontology analysis (biological process) of genes with (*B*) increased expression, UP genes, or (*C*) decreased expression, DOWN genes due to *Apobec2* knockdown prior to differentiation induction (day 0) and postdifferentiation induction (day 1 and day 2). The gene list was filtered, *P*-adjusted < 0.05 and absolute log2 fold change > 0.6, from the list of differentially expressed genes at each time point. Color gradient represents decreasing *P*-adjusted values; dot size represents increasing Gene Ratio. Analysis and plots were done using compareCluster function of clusterProfiler package. (*D*) Plots of normalized read counts (DESeq2) across timepoints (day 0, day 1, and day 2) of *Apobec2* and selected differentially expressed genes. Individual points represent replicates, n = 3.

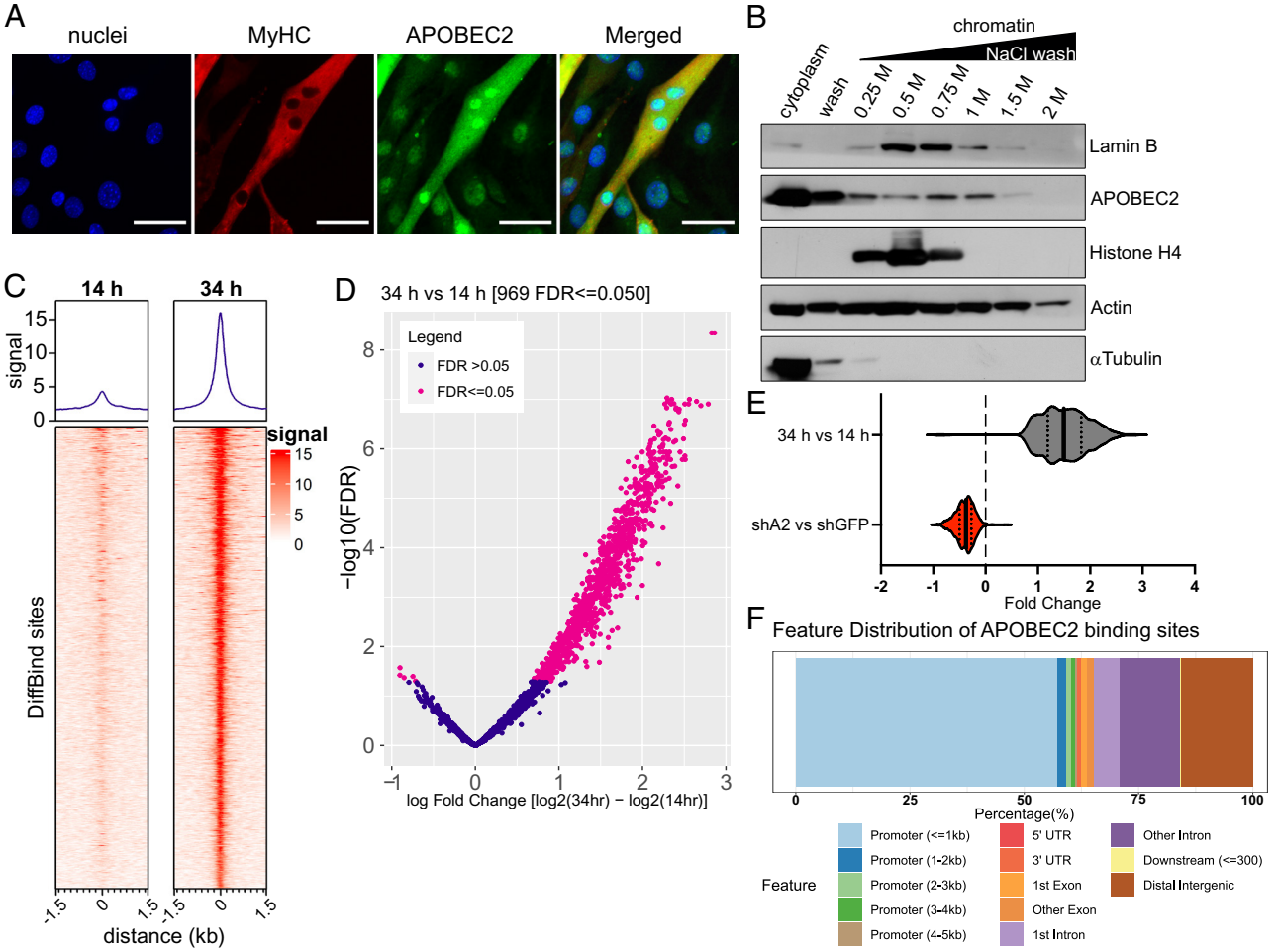

Fig. 3. APOBEC2-occupied promoters of skeletal muscle and nonskeletal muscle genes. (*A*) Immunostaining of APOBEC2 in differentiated C2C12 myoblasts, 5 d postdifferentiation induction. Samples were stained for MyHC (red), APOBEC2 (green), and nuclei (DAPI, blue). (Scale bar, 50 μm.) (*B*) The sequential salt extraction profile of endogenous APOBEC2, lamin B, histone H4, beta-actin, and alpha-tubulin. The relative amount of indicated proteins in corresponding eluates was measured by western blotting. (*C*) ChIP signal within APOBEC2-binding sites at 14 h and 34 h time points postdifferentiation induction. A summary plot showing the average signal across all sites is present above the corresponding heatmaps. Signal was calculated from normalized read counts within 1.5 kb pairs upstream and downstream of the summit of each peak. Each line of the heatmap defines an APOBEC2-binding site. A total of 2,168 consensus sites, defined as binding sites called in at least 2 samples across both time points (2 out of 6 samples, three biological replicates per time point). (*D*) Volcano plot of APOBEC2 peaks with log2 fold changes and *P*-adjusted (false discovery rate, FDR). Each point represents a peak, peaks in pink fall within the FDR cutoff < 0.05. (*E*) Summary violin plots of fold changes of APOBEC2 peaks between 34 h and 14 h in the control (shGFP) samples and between Apobec2 knockdown (shA2) and shGFP at 34 h. Violin plot shape represents the distribution of the data; solid line, median; dotted lines, quartile. (*F*) Genomic annotations of APOBEC2 differentially bound sites 14 h and 34 h postdifferentiation induction. Binding regions are annotated based on genomic feature (UCSC mm10). The priority of assignment to a genomic feature when there is annotation overlap is Promoter (−5, +2 kb TSS), 5′ UTR, 3′ UTR, Exons, Introns, Downstream, and Distal Intergenic.

of low and higher APOBEC2 protein abundance. Overall, the signal around peak summits of APOBEC2 was higher at 34 h vs. 14 h, reflecting an increase of APOBEC2 in chromatin and correlating to the increase in APOBEC2 expression levels (Fig. 3*C*). We then defined a list of APOBEC2 target sites by using the DiffBind R package (43), which compares the signal (ChIP-Seq read counts) at the called peaks between the time points. Of the 969 sites that had differential APOBEC2 occupancy (fdr ≤ 0.05), 964 had increasing signal at the 34 h time points (Fig. 3*C* and Dataset S3). The mean fold change increase across these sites was 1.5 (Fig. 3 *D* and *E*). Moreover, upon knockdown of APOBEC2, there was a decrease in signal at these sites with a mean fold change decrease of 0.39 (Fig. 3*E*). The partial abolishment of APOBEC2 binding at these sites was due to the incomplete removal of APOBEC2 protein in the mRNA knockdown cells. We focused on these sites where signal increased as APOBEC2 protein levels increased with differentiation; suggesting that these sites were biologically relevant.

Annotating the APOBEC2 sites by genomic feature showed that for both time points most of the sites fall within promoters, defined as regions −5 kilobases (kb) to +2 kb around the TSS (Fig. 3*F*). This suggested that APOBEC2 might play a role in the transcriptional regulation of the genes linked to these promoters. Additionally, we did not observe APOBEC2-related DNA mutation at the occupied peaks, indicating that APOBEC2 was not a DNA mutator like other APOBEC family members (*SI Appendix*, Fig. S3).

Promoter-Bound APOBEC2 Affected Expression of Nonskeletal Muscle Genes. We next annotated the APOBEC2 sites to the nearest genes on the mouse genome (mm10 UCSC) transcript database to uncover which genes were potentially regulated by APOBEC2 during myoblast to myotube differentiation. Using gene ontology analysis, the APOBEC2 target genes were enriched for genes involved in muscle cell differentiation and, unexpectedly, hemopoiesis and myeloid cell differentiation (Fig. 4*A* and Dataset S4). Next, we determined whether APOBEC2 occupancy affected the expression of these specific cell differentiation target genes (Fig. 4*B*). Several APOBEC2 target muscle differentiation genes were differentially expressed when APOBEC2 was knocked down. Among them was *Akap6*, described earlier as a kinase involved in cytoskeletal rearrangements during muscle

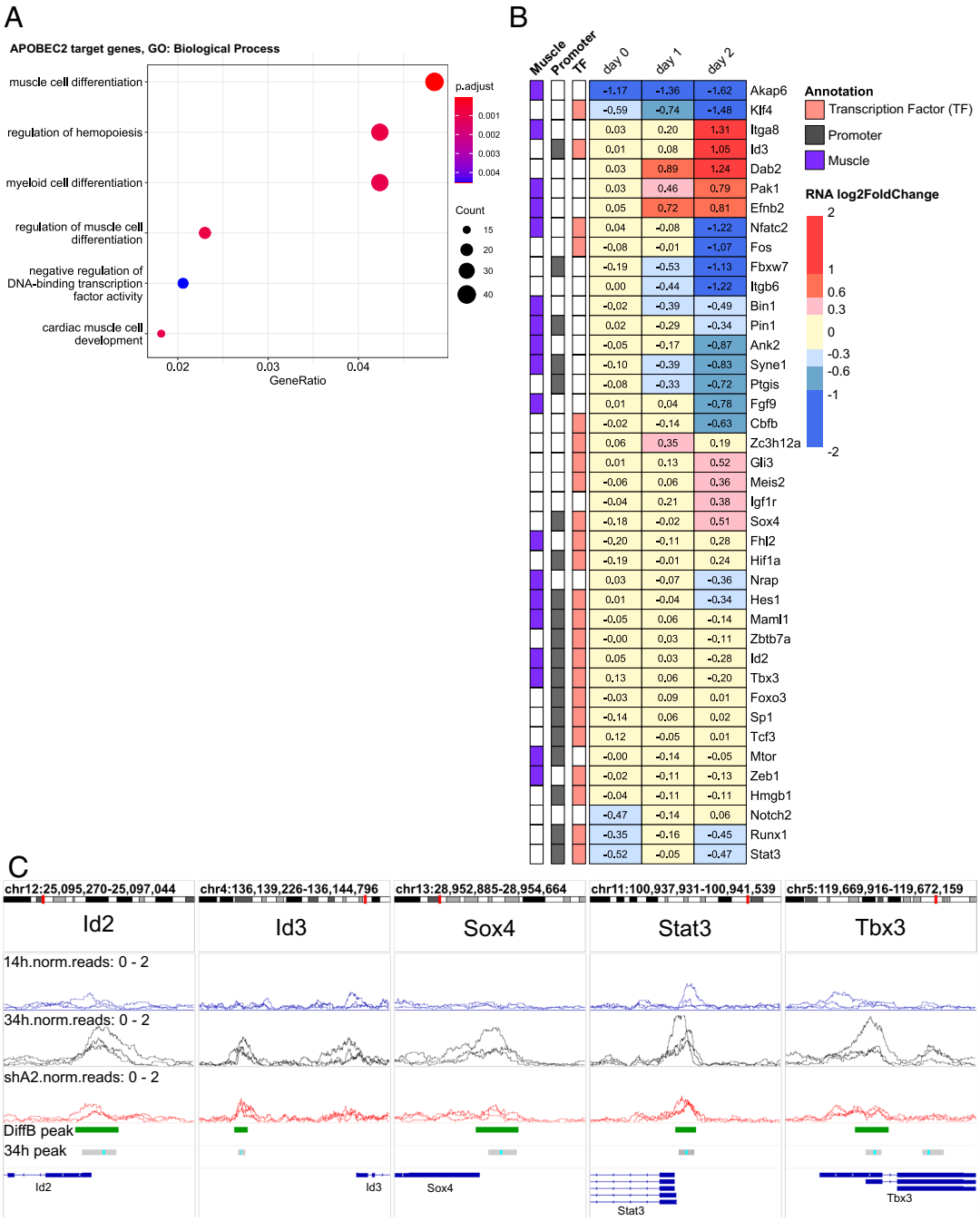

Fig. 4. APOBEC2-occupied genes changed expression during muscle differentiation. (*A*) Gene ontology analysis of APOBEC2 target genes. The target gene list was taken from the APOBEC2 target sites, FDR < 0.05, annotated to the nearest gene (mm10 UCSC). Color gradient represents decreasing *P*-adjusted values; dot size represents increasing gene count. (*B*) Heatmap representing gene expression changes of APOBEC2 target genes. The gene list was filtered from GO terms on (*A*). Genes were annotated as "Muscle" belong to the muscle-related GO terms; as "Promoter" are promoter-bound (−5, +2 kb transcription start site); and as "Transcription Factors." Values represent log2FoldChange of shA2 vs. shGFP RNA-Seq at the specified timepoints (day 0, day 1, and day 2). Colors represent log2FoldChange between specified breaks, reds = increased and blues = decreased gene expression. (*C*) Gene tracks of APOBEC2 ChIP-Seq reads at specified genes from early differentiating C2C12 myoblasts, 14 h and 34 h, and the APOBEC2 knockdown C2C12 myoblast (snap from Integrative Genomics Viewer, IGV). Normalized read counts are represented as line plots of triplicates, range: 0 to 2. DiffBind and representative MACS2 peak calls are marked by bars. Gene exons and introns are annotated with lines and bars according to the mm10 genome assembly.

differentiation with decreased expression in the steady-state (day 0) APOBEC2 knockdown cells. This suggested that APOBEC2 binding at *Akap6* was consequential to its gene expression even though APOBEC2 occupancy was not at its promoter region. Interestingly, APOBEC2-occupied transcription factors involved in both muscle and nonmuscle cell fates. Several nonmuscle transcription factors showed increased expression with APOBEC2 knockdown (e.g., *Id3*, *Zc3h12a*, *Gli3*, *Meis2*, and *Sox4*, genes involved in blood cell fates) suggesting a perturbed myogenic cell fate in the knockdown C2C12 cells. Notably, we found that APOBEC2-occupied promoter regions of the *Sox4* and *Id3* genes (known inhibitors of muscle differentiation) (44) suggesting a direct role for APOBEC2 in the transcriptional regulation of these genes (Fig. 4 *B* and *C*) as well as a potential mechanism for the upregulation of non-skeletal-muscle-related genetic pathways observed in the APOBEC2 knockdown C2C12 cells. We conclude that APOBEC2 acts as a transcriptional repressor to direct C2C12 differentiation into the muscle lineage by repressing these specious

gene networks related to other lineages—counteracting the known promiscuity of muscle identity transcription factor, *Myod1* (45).

APOBEC2 Binds Directly to Single-Stranded DNA in a Sequence-Specific Manner. Thus far, the results suggest that APOBEC2 has a molecular role unique to the APOBEC family. While it does not have the capacity to modify nucleic acids (RNA or DNA) through deamination, we have shown that it was capable of binding chromatin to regulate transcription. This implies either that APOBEC2 interacts directly with DNA at promoter regions, or that it interacts with transcription regulators that do so, or both.

The members of the APOBEC family that bind to DNA have some local sequence preference with regard to sites they mutate but do not display rigorous sequence specificity akin to TF-binding sites (46). We used STREME motif enrichment analysis to determine motifs enriched at the APOBEC2-binding sites at the target gene promoter regions (47). The top enriched motif found at 82% of the sites was a GC-rich motif (Fig. 5*A*), potentially recognized by the SP Specificity protein 1-like factors (SP)/Krüppel-like factor (KLF) transcription factor family (48). To assess whether APOBEC2 is capable of binding DNA directly at those sites, we generated recombinant mouse APOBEC2 and asked whether it could bind this GC-rich SP/KLF motif in vitro (using an A-tract motif as a potential negative control). To measure binding we used microscale thermophoresis (MST), an in vitro method that measures the affinity of two potentially interacting molecules from changes in their movement, tracked through fluorescence shifts, in solution when heat is applied (49). As an additional control we used a variant of APOBEC2 with a point mutation on the catalytic pocket, E100A; the homologous mutation in AID (E58A) disrupts catalytic activity and binding (50). We labeled recombinant APOBEC2 with a fluorescent tag, Cy5, and first measured shifts in fluorescence, ΔFnorm, for the wild-type protein in the presence of both motifs (SP/KLF and poly-A. While wild-type protein bound directly to both motifs (Fig. 5 *B* and *C*), APOBEC2 E100A showed no characteristic curve in the fluorescent shift, which indicated that the mutation abrogated the binding to either motif (Fig. 5 *B* and *C*). APOBEC2 bound the SP/KLF motif with 20-fold stronger affinity than the control poly-A motif, 926.48 ± 243.48 nM vs. 20,213 ± 6,575.4 nM (Fig. 5*D*), suggesting that SP/KLF was indeed preferred. The measured affinity, 0.9 μM, was within the range of estimated affinities for other APOBEC members for their known cognate ligands, e.g., 0.6 μM for APOBEC1 (51). These data demonstrate that APOBEC2 can bind DNA in a sequence-specific manner, in vitro and in vivo (ChIP-Seq), at promoter regions–a key characteristic of transcriptional regulators.

APOBEC2 Interacted with Corepressor Complexes In Vivo. Binding of recombinant APOBEC2 to DNA suggested that it can bind directly to chromatin at promoter regions—but how would it repress transcription? We wondered whether, in vivo, APOBEC2 recruited cofactors to promoter regions that would enforce transcriptional repression. To query such cofactors we used proximity-dependent protein biotinylation (BioID). After statistical curation we identified 124 proteins that were significantly more tagged by APOBEC2-BirA and/or BirA-APOBEC2 than GFP-BirA controls in C2C12 cells (Dataset S5). Functional annotation showed that many APOBEC2 neighboring proteins are related to cell membrane and cytoskeleton organization processes, in line with its high cytoplasmic abundance (Fig. 3*A*), but terms related to chromatin modification and histone deacetylation were also enriched (*SI Appendix*, Fig. S4*A* and Dataset S5). Of particular significance was the identification the HDAC1 and Chromodomain-helicase-DNA-binding protein 4 (CHD4), key components of

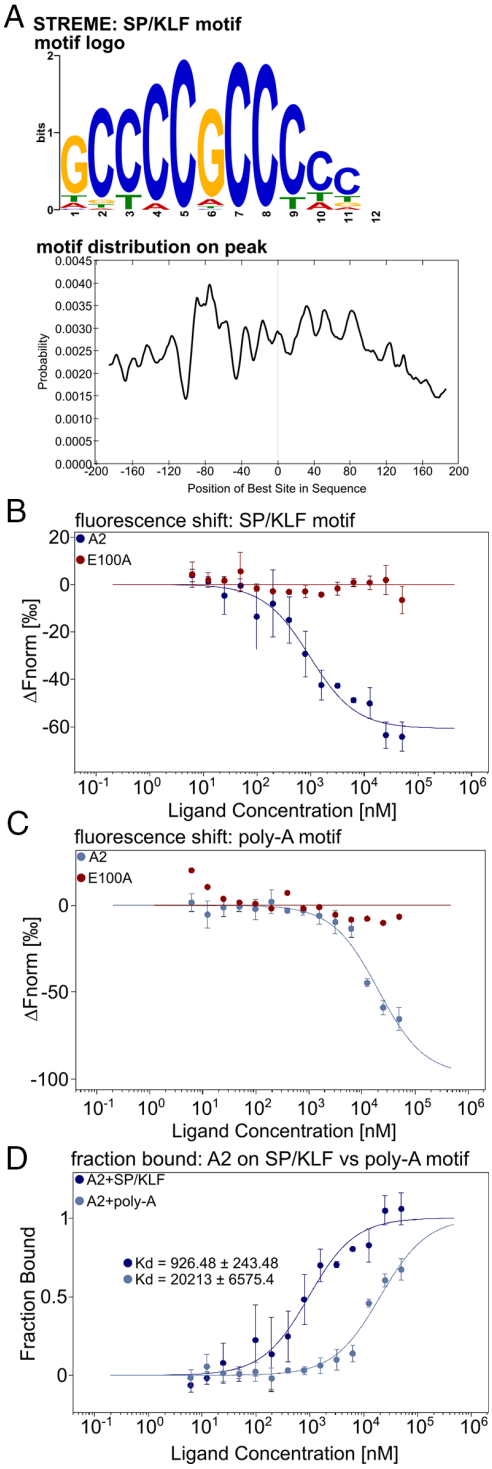

Fig. 5. APOBEC2 peaks at promoter regions were enriched for an SP/KLF motif. (*A*) APOBEC2 peaks found on promoters of target genes centered at the summit, ±200 bp, were used for motif discovery analysis, STREME (47). The identified GC-rich motif was matched to several SP/KLF transcription factor motifs, using the Tomtom motif comparison tool with HOCOMOCO v11 full database. Peaks were centrally enriched as plotted by Centrimo, line plot below motif logo. (*B* and *C*) Fluorescence shift plot from MST experiments measuring purified APOBEC2 binding to single-stranded DNA with an (*B*) SP/KLF motif or (*C*) poly-A motif. Cy5-labeled APOBEC2 (blue) or APOBEC2 E100A mutant (E100A, red) was kept constant (50 nM) while the concentration of nonlabeled SP/KLF motif was titrated between 10 and 20,000 nM. Points and error bars represent the mean normalized fluorescence shift (ΔFNorm) and SD from three replicates. Curve fitting was done using the Kd model of the MO.Affinity Analysis v2.1 software. (*D*) Fraction-bound plot derived from fluorescence shift plots for APOBEC2 on the SP/KLF motif (blue) and poly-A motif (light blue) with calculated Kd values. The Kd was calculated using the MO.Affinity Analysis v2.1 software.

the nucleosome remodeling and histone deacetylation (NuRD) transcriptional corepressor complex 32, (Fig. 6*A* and *SI Appendix*, Fig. S4*B*). Using coimmunoprecipitation (co-IP), we validated that APOBEC2 interacts with HDAC1 and CHD4 in differentiated C2C12 myoblasts (Fig. 6*B*). Together with the observation that APOBEC2 interacts directly with chromatin, this suggests that APOBEC2 plays a role in gene regulation through epigenetic nucleosome modification with these transcriptional corepressor complexes.

Loss of APOBEC2 Led to Increased Histone Acetylation at the Promoter of *Id3*. Among the differentially expressed APOBEC2 target genes, we decided to investigate the role of APOBEC2 in *Id3* regulation as it inhibits muscle differentiation and is involved in the differentiation of other cell fates. Moreover, the APOBEC2 binds the *Id3* promoter and contains an SP/KLF-motif, suggesting that the DNA binding we measured in vitro is of biological relevance. To assess APOBEC2 occupancy on the *Id3* promoter we expressed FLAG-tagged APOBEC2 in C2C12 myoblasts and performed ChIP (using a ChIP-grade anti-FLAG antibody). Knowing that most APOBEC2 is cytoplasmic, and to increase the ChIP signal, we attached a NLS to APOBEC2 for comparison. We also included its E100A variant as a negative control. Using ChIP-qPCR we confirmed that APOBEC2 binds to the *Id3* promoter containing the SP/KLF motif (Fig. 7*B*). Moreover, APOBEC2 binding to the *Id3* promoter was increased with NLS-APOBEC2 as would be expected from a protein that interacts with chromatin at promoters. And finally, the non-DNA-binding E100A had a lower signal, which validated what we observed in vitro through MST. These observations were similar at other SP/KLF containing APOBEC2 target genes (e.g., *Id2* and *Stat1*).

Finally, we directly assessed the biological relevance of the interaction between APOBEC2 and the HDAC corepressor complex through measuring histone 3 lysine 27 acetylation (H3K27ac) levels at APOBEC2 target genes. Using qPCR, we measured an increase in H3K27ac signal at sites flanking the APOBEC2-binding site on the *Id3* gene (Fig. 7*C*). This provided direct evidence that APOBEC2 binding leads to transcriptional regulation of *Id3* through histone deacetylation. H3K27ac levels were also moderately affected at other APOBEC2 target sites on *Id2* and *Stat1*. Our results suggest a direct role for APOBEC2 in transcriptional regulation, mediated by the NuRD corepressor complex during C2C12 myoblast differentiation (*SI Appendix*, Fig. S5).

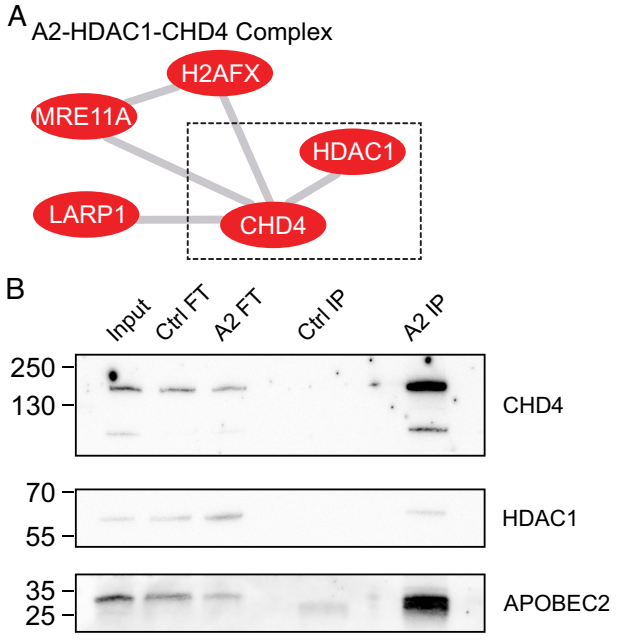

Fig. 6. APOBEC2 recruits the HDAC1 cotranscriptional repressor complex. (*A*) Selected protein complex identified by APOBEC2 proximity-dependent protein biotinylation (BioID). Each red node corresponds to a protein that was identified by BioID mass spectrometry to interact with APOBEC2. CHD4 was also identified in BioID data comparing APOBEC2 and AID in mouse B cells (52). The edges denote the known interactions of these proteins with each other (see *SI Appendix*, Fig. S4*B* for other complexes). (*B*) Co-IP of APOBEC2 with HDAC1 and CHD4 in C2C12 myoblasts to myotubes, differentiation for 4 d. Nuclear protein lysates (Input) treated with nuclease were incubated with beads conjugated to either APOBEC2 antibody (A2 IP) or IgG isotype control antibody (Ctrl IP). Ctrl and A2 flowthrough (FT) were also blotted. Proteins were then eluted, ran on an SDS-PAGE gel, and blotted with APOBEC2, HDAC1, or CHD4 antibodies.

Discussion

There have been many hypothesized roles for the cytidine deaminase APOBEC2. Here, we show that the expression of APOBEC2 during myoblast differentiation has consequences on myotube formation owing to at least one unexpected molecular function: transcriptional control. We found that APOBEC2 loss leads to disrupted myoblast differentiation and concomitant gene expression changes. We show that these gene expression changes may come about through direct chromatin interaction of APOBEC2 at promoters—with no observed APOBEC2-related changes in RNA editing, DNA methylation, or DNA mutation. We found instead that APOBEC2 is capable of directly binding DNA within specific motifs, and directly interacting with corepressor complexes. Together, these interactions provide a mechanistic view on how APOBEC2 can act as a transcriptional regulator of muscle differentiation.

The deaminase domain of APOBEC2 appears to have lost catalytic activity (55, 56). However, we show that it has retained its ability to bind nucleic acids similar to how other APOBEC proteins bind their nucleic acid substrates (57). Demonstrating that APOBEC2 interacts with chromatin through DNA binding is unreported for other members of the APOBEC family. Prior work has linked APOBEC2 overexpression to RNA editing of specific transcripts as observed in the healthy livers of transgenic mice which develop hepatocellular carcinoma (18). Notably, RNA editing was only detectable in the liver at specific transcripts of the mice. However, based on our transcriptome analysis, we were unable to find evidence of such RNA editing in myoblast differentiation. Prior work has also reported mild effects of APOBEC2 on DNA methylation specifically at the *Myog* promoter (25); yet from our ChIP-Seq data, we do not find promoter occupancy of the *Myog* gene. Furthermore, there are conflicting data on the role of the APOBEC family in active DNA demethylation, and APOBEC2-dependent demethylation has not been found in other cellular contexts (58, 59). A role in transcriptional regulation, such as we propose, would explain these prior findings as indirect effects of disrupted cell differentiation and identity due to dysregulated transcriptional programs.

Previous studies suggested that recombinant APOBEC2 is incapable of binding DNA (55, 56). Our experiments using recombinant protein produced in eukaryotic cells show that APOBEC2 was capable of binding DNA with comparable affinity to other APOBEC members. Interestingly, zebrafish homologs of APOBEC2, Apobec2a and 2b, have been shown to increase binding of the transcription factor POU6F2 to an OCT1 motif, although APOBEC2 itself was not shown to bind to the motif (21). Together, our findings suggest that APOBEC2 might play both a direct and indirect role in transcriptional regulation through directly binding DNA or altering transcriptional regulator affinity for cognate motifs.

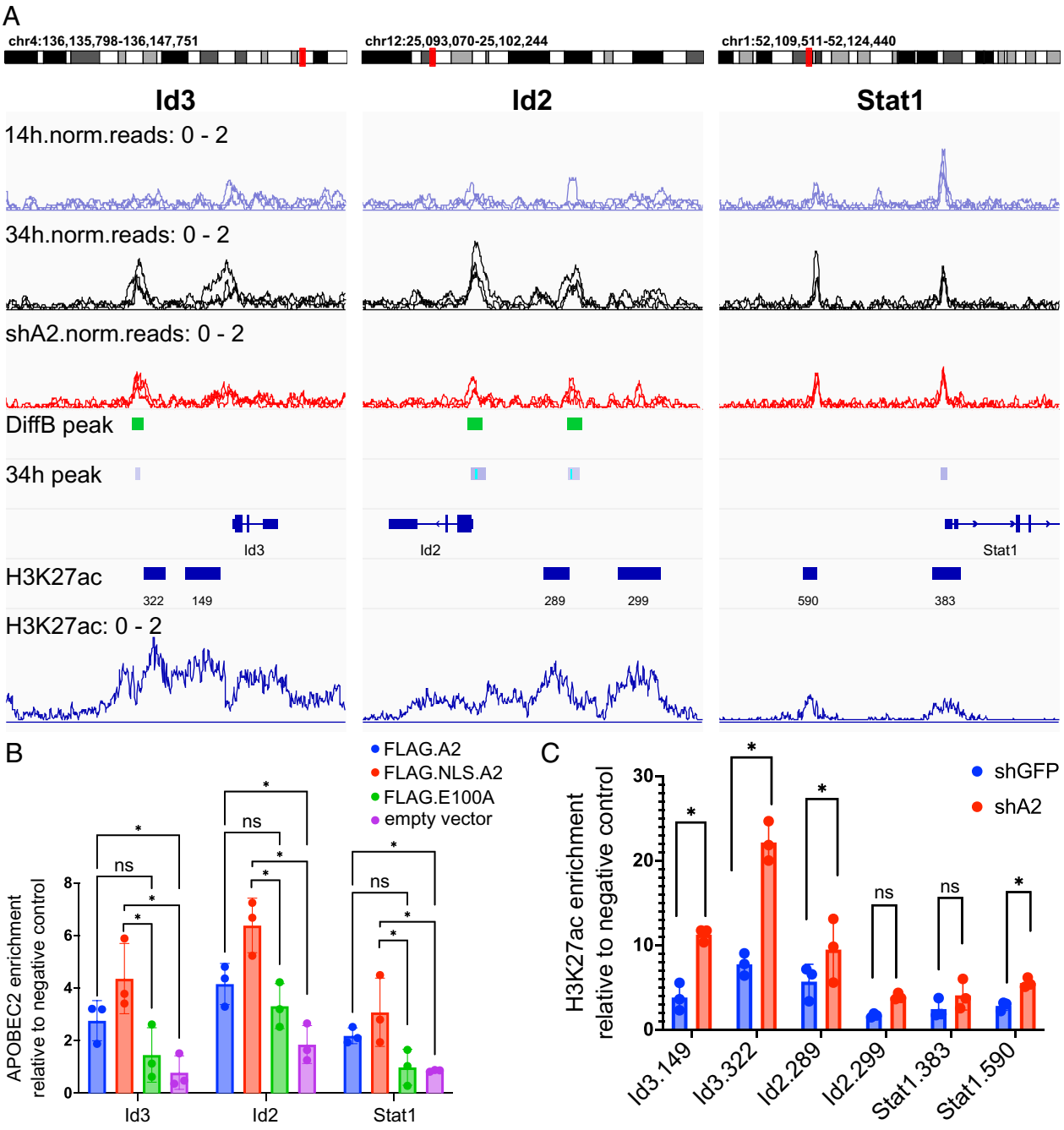

Fig. 7. Histone H3 lysine 27 acetylation at sites proximal to APOBEC2 target sites was decreased with APOBEC2 knockdown. (*A*) APOBEC2 ChIP-Seq tracks at specified genes from early differentiating C2C12 myoblasts, 14 h and 34 h, and the APOBEC2 knockdown C2C12 myoblast (snap from Integrative Genomics Viewer, IGV). ChIP tracks are represented as line plots of normalized read counts of triplicates, range: 0 to 2. H3K27ac ChIP tracks were taken from an experiment with C2C12 myoblasts (GEO: GSE76010) (53) accessed using ChIP-Atlas: SRX1482272 (54). DiffBind and representative peak calls are marked by bars. Gene exons and introns are annotated with lines and bars according to the mm10 genome assembly. (*B*) Stable C212 cell lines were generated using viral transduction introducing distinct variants of APOBEC2 with N-terminal FLAG tags. The variants included FLAG.A2, representing wild-type mouse APOBEC2; FLAG.NLS.A2, featuring an additional N-terminal NLS (SV40 large T antigen); and FLAG.E100A, a mutant APOBEC2 variant characterized by compromised DNA-binding affinity. An empty, vector only, was used as a negative control. The bar plots are from a ChIP qPCR that represent the enrichment of APOBEC2 binding on the sequences of genes previously identified as APOBEC2 target sites with the anti-APOBEC2 ChIP. ChIP was done with anti-FLAG antibody on C2C12 cells differentiated for 34 h (n = 3 independent replicates). An anti-rabbit isotype antibody was used as a negative control. Data were normalized to a genomic region outside the target site. Significance, denoted by asterisks (*), reflects adjusted *P*-values below 0.05, as determined through a two-way ANOVA with corrections for multiple comparisons using Tukey's method, ns, not significant. The data passed the normality distribution test, specifically the Shapiro–Wilks test. (*C*) Barplots represent the enrichment of H3K27ac from a ChIP experiment, measured by qPCR. ChIP was performed on the APOBEC2 knockdown (shA2) and control (shGFP) C2C12 cell lines (n = 3 independent replicates). The primers for the qPCR were designed to amplify proximal H3K27ac (shown in Fig. 3*A*). A negative control region outside of the APOBEC2 target site and without H3K27ac was the negative control. Significance, denoted by asterisks (*), corresponds to adjusted *P*-values below 0.05, determined through a two-way ANOVA with corrections for multiple comparisons utilizing Tukey's method. The data passed a normality distribution test (Shapiro–Wilks).

Uniquely among APOBEC family members, the aminoterminus of APOBEC2 contains a region that is glutamate-rich and intrinsically disordered (27). We showed that deletion of this unstructured domain resulted in the inability of the protein to rescue the knockdown phenotype likely through the loss of its nuclear retention. Given the structural similarity of the cytidine deaminase domain of APOBEC2 to other single-domain APOBEC family members, detrimental changes to the folding of the deaminase

domain by deletion of this disordered accessory domain would be unlikely. Moreover, similarly truncated APOBEC2 shows proper folding in a crystal structure (26). It is likely that the deletion led to disruption of APOBEC2 intramolecular interactions as previously hypothesized (27). Proteins with similar disordered domains form liquid phase separated membrane-less compartments though inter- and intramolecular interactions mediated by this accessory domain (60). Interestingly, such disordered domains are also found in transcriptional regulators (61). It is interesting to speculate that the disordered domain of APOBEC2 also mediates its role in transcriptional regulation through intramolecular interactions in phase-separated transcriptional compartments.

Moreover, our protein interaction experiments revealed that APOBEC2 protein directly interacts with the HDAC1 and CHD4 containing NuRD corepressor complex. This provides a direct epigenetic mechanism through deacetylation for the regulation of APOBEC2-occupied genes. Interestingly, the NuRD corepressor complex is involved in fate determination between skeletal or cardiac muscle (62). Moreover, CHD4 has a direct role in cell fate maintenance during skeletal muscle regeneration, which links epigenetic regulation to the disrupted muscle phenotype observed in the APOBEC2 knockout mice (63). Our data showed that APOBEC2 occupies genes related to nonskeletal muscle though APOBEC2 reduction did not significantly alter their expression. Perhaps in a less skeletal muscle committed cell, one might observe strong upregulation of these genes with APOBEC2 reduction. This implies that APOBEC2 might serve a role in the differentiation of other cellular fates (e.g., T cells, where it is also highly expressed).

Broadly speaking, given the specificity of APOBEC2 expression in muscle cells, both skeletal and cardiac, and the evidence for its role as a transcriptional regulator, we hypothesize that APOBEC2 acts as a modulator of muscle differentiation through repression of nonmuscle programs. We showed that APOBEC2 in differentiating skeletal myoblasts occupies non-skeletal-muscle-related genes. The occupied genes were involved in myocardial or immune cell differentiation, which are different fates of the mesodermal germ layer. Interestingly, the muscle-specific pioneer transcription factor MYOD1 has been shown to bind and activate lineage programs outside the muscle lineage; however, this is mitigated by corepressors (45). Perhaps APOBEC2 plays a role in the modulation of the promiscuous binding of MYOD1 during skeletal muscle differentiation through recruitment of NuRD corepressor complexes at nonskeletal muscle targets. A similar role has been defined for MYT1L in neuronal differentiation, where MYT1L acts as a safeguard of the neuronal fate through repression of non-neuronal cell fates (64).

The finding that APOBEC2 has a direct role in transcriptional control impacts how we interpret the phenotypes that have been attributed to it in the mouse knockout models and other biological systems, well beyond muscle differentiation—for example, zebrafish retina and optic nerve regeneration, *Xenopus* embryo development, and cancer development (14, 15, 18). In the zebrafish models, APOBEC2 loss leads to similar defective muscle phenotypes, but it is deemed essential in the retinal regeneration model—where cellular reprogramming is a key step (14). Perhaps our observation of increased centrally nucleated fibers in the uninjured APOBEC2 knockout mice was indicative of premature activation of muscle satellite cells, which was also a proposed mechanism for the accelerated but faulty differentiation of mouse primary myoblasts (65). Directly or indirectly, these prior observations likely relate to aberrant transcriptional programs, normally regulated in the context of tissue development or cell differentiation by APOBEC2 transcriptional control. Taken together, our data demonstrate that APOBEC2 functions as a transcriptional repressor that modulates specific transcriptional programs during cell differentiation.

In the context of the APOBEC family of deaminases and their molecular evolution, ancient APOBEC2 branches out from AID and the rest of the bona fide deaminases (8). APOBEC2 may have lost its ability to deaminate a nucleic acid substrate to preserve genetic stability due to its co-opted role as a transcriptional regulator. Its characteristic N-terminal flexible region may be a structural signpost to its role in transcriptional regulation. APOBEC2 is an APOBEC member without the ability to change genetic information, but it plays a role in the epigenetic regulation of cell fate.

Materials and Methods

Datasets. High-throughput sequencing datasets are all found in GSE117732 and more specifically RNA-Seq (GSE117730); ChIP-Seq (GSE117729); and ERRBS (GSE117731). Mass spectrometry data for BioID performed in Flp-In 293 T-REx cells have been deposited in MassIVE under ID (to be submitted by the JMDN group).

RNA Expression Analysis. Library preparation and sequencing were done by Rockefeller University Genomics Resource Center (https://www.rockefeller.edu/genomics/) using the TruSeq Stranded mRNA Sample Prep kit as per the manufacturer's instruction. Libraries were sequenced with 50 bp paired-read sequencing on the HiSeq2500 (Illumina). Paired-end read alignments and gene expression analysis were performed with the Bioinformatics Resource Center at Rockefeller University. Paired-end reads were aligned to mm10 genome using the subjunc function in the Bioconductor Rsubread package (66). For analysis of differential expression, transcript quantifications were performed using Salmon (67). Gene expression changes were identified at a cutoff of padj < 0.05 in DESeq2 (68). Annotation files used were BSgenome.Mmusculus.UCSC.mm10 (v1.4.0); org.Mm.db (v3.5.0); and TxDb.Mmusculus.UCSC.mm10.knownGene.gtf.gz (v3.4.0). ClusterProfiler/enrichGO (v4.0.5) (69) was used for gene ontology overrepresentation analysis, GO biological processes.

APOBEC2-Deficient Mice. APOBEC2-deficient (*Apobec2−/−*, APOBEC2 KO) mice were provided by Lawrence Chan (Baylor College of Medicine, Houston, TX). The strain carries a null mutation of Apobec2 due to a *neo* cassette insertion into exon 2. The strain of origin was 129P2/OlaHsd and fully backcrossed into C57BL/6. All mice were bred and maintained at the Rockefeller University Animal Care Facility and in accordance with the Rockefeller University Animal Care and Use Committee.

Muscle Tissue Cryosection, Staining, and Image Analysis. Frozen and optimal cutting temperature compound (OCT)-embedded TA muscles from 10-wk-old mice were cut to 10 μm thick cross-sections, air-dried, and stained with Wheat Germ Agglutinin, Alexa Fluor 488 Conjugate (1 μg/mL), and DAPI (1 μg/mL). For each TA muscle cross-section, three nonoverlapping sections (close to the muscle center) were acquired and quantified with ImageJ macros.

Detailed methods on all other molecular and cellular experiments reported herein are available in *SI Appendix*, *Materials and Methods* section.

Data, Materials, and Software Availability. High throughput sequencing datasets, RNA-Seq, ChIP-Seq, ERRBS, and Mass spectrometry data have been deposited in GEO (GSE117732 (70), GSE117730 (71), GSE117729 (72), and GSE117731 (73) and MassIVE (MSV000094388, https://doi.org/10.25345/C58K75735) (74)). All other data are included in the manuscript and/or supporting information.

ACKNOWLEDGMENTS. This work is supported through funding by the Helmholtz Foundation to the DKFZ (F.N.P.) and by a Deutsche Forschungsgemeinschaft (German Research Foundation)–project number 439669440 TRR319 RMaP TP A04 to C.D. and F.N.P. Financial support was also provided through the David Rockefeller Graduate Program (L.M.). Work in the J.M.D.N. lab is supported by

the Canadian Institutes of Health Research grant PJT 155944. J.M.D.N. in a merit scholar from The Fonds de recherche du Québec–Santé.

Author affiliations: [a]Division of Immune Diversity, German Cancer Research Center, Heidelberg 69120, Germany; [b]Faculty of Biosciences, Heidelberg University, Heidelberg 69120, Germany; [c]Laboratory of Lymphocyte Biology, The Rockefeller University, New York, NY 10065; [d]Structural and Computational Biology Unit, European Molecular Biology Laboratory, Heidelberg 69117, Germany; [e]Institute of Computational Biology, Helmholtz Zentrum München, German Research Center for Environmental Health, Neuherberg 85764, Germany; [f]Institut de Recherches Cliniques de Montréal, Montréal, QC H2W 1R7, Canada; [g]Department of Medicine, Division of Experimental Medicine, McGill University, Montréal, QC H4A 3J1, Canada; [h]Department of Biology, Nazareth University, Rochester, NY 14618; [i]Department of Medicine, Université de Montréal, Montréal, QC H3C 3J7, Canada; [j]Klaus Tschira Institute for Integrative Computational Cardiology, University Hospital Heidelberg, Heidelberg 69120, Germany; and [k]German Center for Cardiovascular Research (DZHK) - Partner site Heidelberg/Mannheim, Heidelberg 69120, Germany

Author contributions: J.P.L., L.M., E.M.A., J.M.D.N., and F.N.P. designed research; J.P.L., L.M., E.M.A., I.L.I., S.R., C.N., C.G., J.R., P.G.S., J.B., and D.H. performed research; E.M.A., A.V., and J.M.D.N. contributed new reagents/analytic tools; J.P.L., L.M., E.M.A., I.L.I., C.N., C.G., D.H., J.M.D.N., C.D., J.B.Z., and F.N.P. analyzed data; and J.P.L. and F.N.P. wrote the paper.

1. S. G. Conticello, The AID/APOBEC family of nucleic acid mutators. *Genome Biol.* **9**, 229 (2008).
2. R. Pecori, S. Di Giorgio, J. Paulo Lorenzo, F. Nina Papavasiliou, Functions and consequences of AID/APOBEC-mediated DNA and RNA deamination. *Nat. Rev. Genet.* **23**, 505–518 (2022).
3. D. C. Cole *et al.*, Loss of APOBEC1 RNA-editing function in microglia exacerbates age-related CNS pathophysiology. *Proc. Natl. Acad. Sci. U.S.A.* **114**, 13272–13277 (2017).
4. V. Rayon-Estrada *et al.*, Epitranscriptomic profiling across cell types reveals associations between APOBEC1-mediated RNA editing, gene expression outcomes, and cellular function. *Proc. Natl. Acad. Sci. U.S.A.* **114**, 13296–13301 (2017).
5. R. S. Harris, J. P. Dudley, APOBECs and virus restriction. *Virology* **479–480**, 131–145 (2015).
6. M. Bochtler, A. Kolano, G.-L. Xu, DNA demethylation pathways: Additional players and regulators. *Bioessays* **39**, e201600178 (2017).
7. P. M. Dominguez, R. Shaknovich, Epigenetic function of activation-induced cytidine deaminase and its link to lymphomagenesis. *Front. Immunol.* **5**, 642 (2014).
8. A. Krishnan, L. M. Iyer, S. J. Holland, T. Boehm, L. Aravind, Diversification of AID/APOBEC-like deaminases in metazoa: Multiplicity of clades and widespread roles in immunity. *Proc. Natl. Acad. Sci. U.S.A.* **115**, E3201–E3210 (2018).
9. S. L. Sawyer, M. Emerman, H. S. Malik, Ancient adaptive evolution of the primate antiviral DNA-editing enzyme APOBEC3G. *PLoS Biol.* **2**, E275 (2004).
10. S. Anant *et al.*, ARCD-1, an apobec-1-related cytidine deaminase, exerts a dominant negative effect on C to U RNA editing. *Am. J. Physiol. Physiol.* **281**, C1904–C1916 (2001).
11. W. Liao *et al.*, APOBEC-2, a cardiac- and skeletal muscle-specific member of the cytidine deaminase supergene family. *Biochem. Biophys. Res. Commun.* **260**, 398–404 (1999).
12. Y. Sato *et al.*, Deficiency in APOBEC2 leads to a shift in muscle fiber type, diminished body mass, and myopathy. *J. Biol. Chem.* **285**, 7111–7118 (2010).
13. C. Etard, U. Roostalu, U. Strähle, Lack of Apobec2-related proteins causes a dystrophic muscle phenotype in zebrafish embryos. *J. Cell Biol.* **189**, 527–539 (2010).
14. C. Powell, F. Elsaeidi, D. Goldman, Injury-dependent Muller glia and ganglion cell reprogramming during tissue regeneration requires Apobec2a and Apobec2b. *J. Neurosci.* **32**, 1096–1109 (2012).
15. A. Vonica, A. Rosa, B. L. Arduini, A. H. Brivanlou, APOBEC2, a selective inhibitor of TGFβ signaling, regulates left-right axis specification during early embryogenesis. *Dev. Biol.* **350**, 13–23 (2011).
16. M. Bierkens *et al.*, Focal aberrations indicate EYA2 and hsa-miR-375 as oncogene and tumor suppressor in cervical carcinogenesis. *Genes Chromosomes Cancer* **52**, 56–68 (2013).
17. J. G. Lohr *et al.*, Discovery and prioritization of somatic mutations in diffuse large B-cell lymphoma (DLBCL) by whole-exome sequencing. *Proc. Natl. Acad. Sci. U.S.A.* **109**, 3879–3884 (2012).
18. S. Okuyama *et al.*, Excessive activity of apolipoprotein B mRNA editing enzyme catalytic polypeptide 2 (APOBEC2) contributes to liver and lung tumorigenesis. *Int. J. Cancer* **130**, 1294–1301 (2012).
19. J. U. Guo, Y. Su, C. Zhong, G. Ming, H. Song, Hydroxylation of 5-methylcytosine by TET1 promotes active DNA demethylation in the adult brain. *Cell* **145**, 423–434 (2011).
20. K. Rai *et al.*, DNA demethylation in zebrafish involves the coupling of a deaminase, a glycosylase, and Gadd45. *Cell* **135**, 1201–1212 (2008).
21. C. Powell, E. Cornblath, D. Goldman, Zinc-binding domain-dependent, deaminase-independent actions of apolipoprotein B mRNA-editing enzyme, catalytic polypeptide 2 (Apobec2), mediate its effect on zebrafish retina regeneration. *J. Biol. Chem.* **289**, 28924–28941 (2014).
22. G. A. Meyer, Evidence of induced muscle regeneration persists for years in the mouse. *Muscle Nerve* **58**, 858–862 (2018).
23. H. M. Blau *et al.*, Plasticity of the differentiated state. *Science* **230**, 758–66 (1985).
24. D. Yaffe, O. Saxel, Serial passaging and differentiation of myogenic cells isolated from dystrophic mouse muscle. *Nature* **270**, 725–727 (1977).
25. E. Carrió *et al.*, Muscle cell identity requires Pax7-mediated lineage-specific DNA demethylation. *BMC Biol.* **14**, 30 (2016).
26. C. Prochnow, R. Bransteitter, M. G. Klein, M. F. Goodman, X. S. Chen, The APOBEC-2 crystal structure and functional implications for the deaminase AID. *Nature* **445**, 447–451 (2007).
27. T. C. Krzysiak, J. Jung, J. Thompson, D. Baker, A. M. Gronenborn, APOBEC2 is a monomer in solution: Implications for APOBEC3G models. *Biochemistry* **51**, 2008–2017 (2012).
28. R. Becker *et al.*, Myogenin controls via AKAP6 non-centrosomal microtubule-organizing center formation at the nuclear envelope. *Elife* **10**, 1–31 (2021).
29. S. W. Lee *et al.*, AKAP6 inhibition impairs myoblast differentiation and muscle regeneration: Positive loop between AKAP6 and myogenin. *Sci. Rep.* **5**, 1–14 (2015).
30. B. Chen, B. H. Han, X. H. Sun, R. W. Lim, Inhibition of muscle-specific gene expression by Id3: Requirement of the C-terminal region of the protein for stable expression and function. *Nucleic Acids Res.* **25**, 423–430 (1997).
31. D. J. Nagel *et al.*, Role of nuclear Ca2+/calmodulin-stimulated phosphodiesterase 1A in vascular smooth muscle cell growth and survival. *Circ. Res.* **98**, 777–784 (2006).
32. Y. O. Lukyanenko *et al.*, Ca2+/calmodulin-activated phosphodiesterase 1A is highly expressed in rabbit cardiac sinoatrial nodal cells and regulates pacemaker function. *J. Mol. Cell. Cardiol.* **98**, 73–82 (2016).
33. Y. Watanabe, Conversion of myoblasts to physiologically active neuronal phenotype. *Genes Dev.* **18**, 889–900 (2004).
34. D. Harjanto *et al.*, RNA editing generates cellular subsets with diverse sequence within populations. *Nat. Commun.* **7**, 12145 (2016).
35. B. Laffleur *et al.*, AID-induced remodeling of immunoglobulin genes and B cell fate. *Oncotarget* **5**, 1118–1131 (2014).
36. K. Chan, D. A. Gordenin, Clusters of multiple mutations: Incidence and molecular mechanisms. *Annu. Rev. Genet.* **49**, 243–267 (2015).
37. S. Kosugi, M. Hasebe, M. Tomita, H. Yanagawa, Systematic identification of cell cycle-dependent yeast nucleocytoplasmic shuttling proteins by prediction of composite motifs. *Proc. Natl. Acad. Sci. U.S.A.* **106**, 10171–10176 (2009).
38. A.-M. Patenaude *et al.*, Active nuclear import and cytoplasmic retention of activation-induced deaminase. *Nat. Struct. Mol. Biol.* **16**, 517–527 (2009).
39. E. G. Porter, K. E. Connelly, E. C. Dykhuizen, Sequential salt extractions for the analysis of bulk chromatin binding properties of chromatin modifying complexes. *J. Vis. Exp.* **128**, 55369 (2017).
40. P. Percipalle, M. Vartiainen, Cytoskeletal proteins in the cell nucleus: A special nuclear actin perspective. *Mol. Biol. Cell* **30**, 1781–1785 (2019).
41. J. Feng, T. Liu, Y. Zhang, Using MACS to identify peaks from ChIP-seq data. *Curr. Protoc. Bioinformatics* **34**, 2.14.1–2.14.14 (2011).
42. Y. Zhang *et al.*, Model-based analysis of ChIP-seq (MACS). *Genome Biol.* **9**, R137 (2008).
43. C. S. Ross-Innes *et al.*, Differential oestrogen receptor binding is associated with clinical outcome in breast cancer. *Nature* **481**, 389–393 (2012).
44. J. Wu, R. W. Lim, Regulation of inhibitor of differentiation gene 3 (Id3) expression by Sp2-motif binding factor in myogenic C2C12 cells: Downregulation of DNA binding activity following skeletal muscle differentiation. *Biochim. Biophys. Acta* **1731**, 13–22 (2005).
45. Q. Y. Lee *et al.*, Pro-neuronal activity of Myod1 due to promiscuous binding to neuronal genes. *Nat. Cell Biol.* **22**, 401–411 (2020).
46. R. M. Kohli *et al.*, Local sequence targeting in the AID/APOBEC family differentially impacts retroviral restriction and antibody diversification. *J. Biol. Chem.* **285**, 40956–40964 (2010).
47. T. L. Bailey, STREME: Accurate and versatile sequence motif discovery. *Bioinformatics* **37**, 2834–2840 (2021).
48. J. Kaczynski, T. Cook, R. Urrutia, Sp1- and Krüppel-like transcription factors. *Genome Biol.* **4**, 206 (2003).
49. C. J. Wienken, P. Baaske, U. Rothbauer, D. Braun, S. Duhr, Protein-binding assays in biological liquids using microscale thermophoresis. *Nat. Commun.* **1**, 100 (2010).
50. Q. Qiao *et al.*, AID recognizes structured DNA for class switch recombination. *Mol. Cell* **67**, 361–373. e4 (2017).
51. A. D. Wolfe, S. Li, C. Goedderz, X. S. Chen, The structure of APOBEC1 and insights into its RNA and DNA substrate selectivity. *NAR Cancer* **2**, 36–38 (2020).
52. S. P. Methot *et al.*, A licensing step links AID to transcription elongation for mutagenesis in B cells. *Nat. Commun.* **9**, 1248 (2018).
53. S. Dell'Orso *et al.*, "The Histone Variant MacroH2A1.2 is Necessary for the Activation of Muscle Enhancers and Recruitment of the Transcription Factor Pbx1." GEO. https://www.ncbi.nlm.nih.gov/geo/query/acc.cgi?acc=GSE76010. Deposited 15 December 2015.
54. Z. Zou, T. Ohta, F. Miura, S. Oki, ChIP-Atlas 2021 update: A data-mining suite for exploring epigenomic landscapes by fully integrating ChIP-seq, ATAC-seq and Bisulfite-seq data. *Nucleic Acids Res.* **50**, W175–W182 (2022).
55. R. S. Harris, S. K. Petersen-Mahrt, M. S. Neuberger, RNA editing enzyme APOBEC1 and some of its homologs can act as DNA mutators. *Mol. Cell* **10**, 1247–1253 (2002).
56. M. C. Mikl *et al.*, Mice deficient in APOBEC2 and APOBEC3. *Mol. Cell. Biol.* **25**, 7270–7277 (2005).
57. J. D. Salter, H. C. Smith, Modeling the embrace of a mutator: APOBEC selection of nucleic acid ligands. *Trends Biochem. Sci.* **43**, 606–622 (2018).
58. C. S. Nabel *et al.*, AID/APOBEC deaminases disfavor modified cytosines implicated in DNA demethylation. *Nat. Chem. Biol.* **8**, 751–758 (2012).
59. C. Powell, A. R. Grant, E. Cornblath, D. Goldman, Analysis of DNA methylation reveals a partial reprogramming of the Muller glia genome during retina regeneration. *Proc. Natl. Acad. Sci. U.S.A* **110**, 19814–19819 (2013).
60. A. Boija *et al.*, Transcription Factors Activate Genes through the Phase-Separation Capacity of Their Activation Domains. *Cell* **175**, 1842–1855 (2018).
61. S. Brodsky *et al.*, Intrinsically disordered regions direct transcription factor in vivo binding specificity. *Mol. Cell* **79**, 459–471.e4 (2020).
62. P. Gómez-del Arco *et al.*, The chromatin remodeling complex Chd4/NuRD controls striated muscle identity and metabolic homeostasis. *Cell Metab.* **23**, 881–892 (2016).
63. K. Sreenivasan *et al.*, CHD4 ensures stem cell lineage fidelity during skeletal muscle regeneration. *Stem Cell Rep.* **16**, 2089–2098 (2021).
64. M. Mall *et al.*, Myt1l safeguards neuronal identity by actively repressing many non-neuronal fates. *Nature* **544**, 245–249 (2017).
65. H. Ohtsubo *et al.*, APOBEC2 negatively regulates myoblast differentiation in muscle regeneration. *Int. J. Biochem. Cell Biol.* **85**, 91–101 (2017).
66. Y. Liao, G. K. Smyth, W. Shi, The Subread aligner: Fast, accurate and scalable read mapping by seed-and-vote. *Nucleic Acids Res.* **41**, e108 (2013).
67. R. Patro, G. Duggal, M. I. Love, R. A. Irizarry, C. Kingsford, Salmon provides fast and bias-aware quantification of transcript expression. *Nat. Methods* **14**, 417–419 (2017).
68. M. I. Love, W. Huber, S. Anders, Moderated estimation of fold change and dispersion for RNA-seq data with DESeq2. *Genome Biol.* **15**, 550 (2014).
69. T. Wu *et al.*, clusterProfiler 4.0: A universal enrichment tool for interpreting omics data. *Innovation (Camb)* **2**, 100141 (2021).
70. L. Molla, F. N. Papavasiliou, D. Harjanto, S. T. Carroll, "A novel role for the conserved, orphan deaminase APOBEC2." GEO. https://www.ncbi.nlm.nih.gov/geo/query/acc.cgi?acc=GSE117732. Deposited 26 July 2018.

71. L. Molla, F. N. Papavasiliou, D. Harjanto, S. T. Carroll, "A novel role for the conserved, orphan deaminase APOBEC2 [RNA-seq]." GEO. https://www.ncbi.nlm.nih.gov/geo/query/acc.cgi?acc=GSE117730. Deposited 26 July 2018.
72. L. Molla, F. N. Papavasiliou, D. Harjanto, S. T. Carroll, "A novel role for the conserved, orphan deaminase APOBEC2 [ChIP-seq]." GEO. https://www.ncbi.nlm.nih.gov/geo/query/acc.cgi?acc=GSE117729. Deposited 26 July 2018.
73. L. Molla, F. N. Papavasiliou, D. Harjanto, S. T. Carroll, "A novel role for the conserved, orphan deaminase APOBEC2 [methylation]." GEO. https://www.ncbi.nlm.nih.gov/geo/query/acc.cgi?acc=GSE117731. Deposited 26 July 2018.
74. J. M. Di Noia, "APOBEC2 Safeguards Skeletal Muscle Cell Fate through Regulating Transcription of Non-Muscle Genes during Myoblast Differentiation." MassIVE. https://massive.ucsd.edu/ProteoSAFe/dataset.jsp?accession=MSV000094388. Deposited 22 March 2024.